

Oxalate Intercalated Mg/Cr Layered Double Hydroxide as Adsorbent of Methyl Red and Methyl Orange from Aqueous Solution

Arini Fousty Badri¹, Novie Juleanti², Neza Rahayu Palapa¹, Yuliza Hanifah³,
Risfidian Mohadi^{2,3}, Mardiyanto⁴, Aldes Lesbani^{1,3*}

¹ Graduate School of Mathematics and Natural Sciences, Universitas Sriwijaya, Jl. Raya Palembang-Prabumulih, Km. 32, Ogan Ilir 30662, South Sumatra, Indonesia

² Department of Chemistry, Faculty of Mathematics and Natural Sciences, Universitas Sriwijaya, Jl. Raya Palembang Prabumulih Km. 32, Ogan Ilir 30662, South Sumatra, Indonesia

³ Research Center of Inorganic Materials and Complexes, Faculty of Mathematics and Natural Sciences, Universitas Sriwijaya, Palembang 30139, Indonesia

⁴ Department of Pharmacy, Faculty of Mathematics and Natural Sciences, Universitas Sriwijaya, Jl. Raya Palembang-Prabumulih, Km. 32, Ogan Ilir 30662, South Sumatra, Indonesia

* Corresponding author's email: aldeslesbani@pps.unsri.ac.id

ABSTRACT

Mg/Cr layered double hydroxide (LDH) has been successfully synthesized by means of the coprecipitation method followed by the intercalation process using oxalate to form Mg/Cr-oxalate. The materials were characterized using XRD, BET, and FTIR and then applied as an adsorbent of anionic dyes i.e. methyl red (MR) and methyl orange (MO). MR and MO adsorption was studied through variations of adsorption time, concentration, temperature, desorption process, and adsorbent regeneration. The XRD characterization results showed an increase in the interlayer distance from 7.62 Å to 11.35 Å after the intercalation process. The increase of interlayer space of Mg/Cr-oxalate is also equal to the BET data, which shows an increase in surface area from 21.511 m²/g to 49.270 m²/g. The kinetics and isotherm parameters of MR and MO adsorption using Mg/Cr LDH and Mg/Cr-oxalate showed the same results following the PFO kinetics model and Langmuir isotherm model with R² close to one. Mg/Cr LDH has the adsorption capacity for MR and MO up to 61.728 mg/g 54.645 mg/g, respectively. In turn, the highest adsorption capacity is achieved by Mg/Cr-oxalate for MR adsorption at 81.235 mg/g and MO at 71.429 mg/g. The thermodynamic parameters of MR and MO adsorption using Mg/Cr LDH and Mg/Cr-oxalate indicate that the adsorption process is endothermic and spontaneous.

Keyword: layered double hydroxide, dyes, adsorption, intercalation, kinetic and thermodynamic

INTRODUCTION

There are more than 100,000 dyes commercially available with more than 107 tonnes of dyes produced annually worldwide. These dyes are widely used by several industries such as foods, cosmetics, paper printings, and the textile industries as the largest dye consumers (Benkhaya et al., 2020). Dyes commonly used in industry can be classified as natural and synthetic dyes. According to Rubia & Bhardwaj, (2016), natural dyes have properties that are

non-toxic, non-carcinogenic, eco-friendly, biodegradable, and easy to dispose of. However, the use of natural dyes is now starting to be replaced by synthetic dyes. Natural dyes are limited and more expensive than synthetic dyes. On the other hand, synthetic dyes are toxic on aquatic environment because of their non-durable, unstable, and lacking color variations (Zhao et al., 2018). Some of the most abundant synthetic dyes are methyl red (MR) and methyl orange (MO). These dyes have an azo functional group (-N=N-) and are classified as anionic dyes (Shan

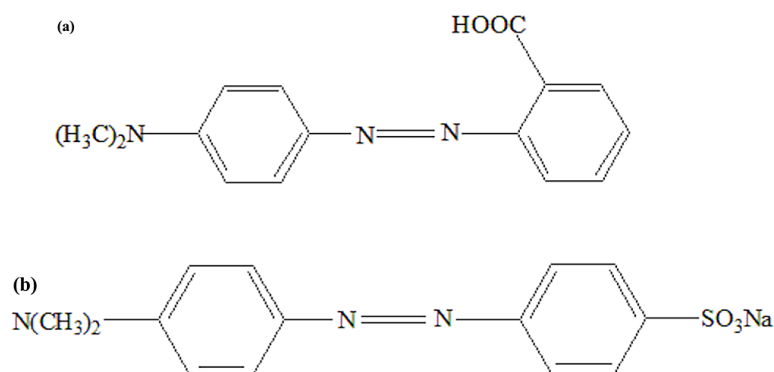


Figure 1. The chemical structures of MR (a) and MO (b)

et al., 2015). The chemical structure of MR and MO can be seen in Figure 1.

Azo dyes are organic compounds that are difficult to biodegrade due to their high stability to light and resistance to microbial attack (He et al., 2018). According to Hassaan & Nemr (2017), this azo dye was found to be complex and is carcinogenic in reductive cleavage. These dyes can change the physical and chemical properties of the soil and water and cause damage to the flora and fauna in the environment. The toxic nature of the dye causes the death of soil microorganisms which in turn affect the agricultural productivity. Therefore, a method to deal with the harmful effects caused by dyes is needed. In recent years, biological, chemical, and physical methods, such as aerobic and anaerobic microbial degradation processes, oxidation, membrane filtration, coagulation, flocculation, flotation, precipitation, and adsorption have been developed to address the dyestuff waste from the environment (Semeraro et al., 2017).

According to Vinsiah et al. (2017), adsorption is one of the most efficient methods to remove liquid waste. The treatment of dyestuff waste by the adsorption method has high effectiveness in removing dyestuffs from wastewater (Amelia & Maryudi, 2019). Imron & Said (2017), revealed that adsorption is considered the most effective technique for removing dyes, due to its simple design, high efficiency, easy handling, and low cost. Various natural and synthetic materials such as activated carbon, graphene, carbon nanotubes, zeolites, polymers, clays, and layered double hydroxides (LDH) can be used as adsorbents for dye removal. However, LDH is favored material because it is easy to synthesize, has high stability, reusability and also modification properties.

LDH is a part of anionic clay with anion-exchange capabilities which can be used as an effective adsorbent to remove various pollutants.

LDH has a general formula $[M^{2+}_{1-x}M^{3+}_x(OH)_2]^{x+}[(A^{n-})_{x/n} \cdot mH_2O]^x$, where M^{2+} and M^{3+} are divalent (Cu^{2+} , Co^{2+} , Ca^{2+} , Zn^{2+} , Mg^{2+} , etc.) and trivalent (Ga^{3+} , Al^{3+} , Fe^{3+} , Cr^{3+} , etc.) metal ions, while A^{n-} is an interlayer anion with charge n (Rathee et al., 2019). One of most interesting properties of LDH is the anion-exchange ability, which can be used to modify the original structure of this material. When the anions in the interlayer are exchanged with other larger anions, the surface area can be increased and the interlayer distances and gallery can be expanded. Some anions that are usually in the interlayer such as nitrate (NO_3^-), sulfate (SO_4^{2-}), chloride (Cl^-), and carbonate (CO_3^{2-}) depending on synthetic conditions (Taher et al., 2019).

Various LDHs have been applied as adsorbent to absorb metal ions or dyes. The results of research Ai et al. (2011), in removing MO dyes using Mg/Al-LDH obtained an adsorption capacity of 0.453 mol/kg. The research conducted by Badri et al. (2021), used intercalated Mg/Cr as adsorbent of Rhodamine B and Methylene blue with the adsorption capacities of 139.526 mg/g and 8.741 mg/g, respectively. The adsorption capacity obtained by (Giscard et al., 2016) in his research to remove nickel ions using intercalated Mg/Cr-oxalate reached 1310 mg/g. Some of these studies prove that modification of LDH has a great ability to remove dye waste.

MATERIALS AND METHODS

Chemicals and instrumentations

The chemicals used in this experiment, included $Mg(NO_3)_2 \cdot 6H_2O$ (Merck, 256.41 g/mol), $Cr(NO_3)_3 \cdot 9H_2O$ (Sigma Aldrich, 400.15g/mol), $C_2H_2O_4 \cdot 2H_2O$ (Merck, 126.07 g/mol), Na_2CO_3 (Merck, 105.88 g/mol), NaOH (Merck, 40.00 g/

mol), HCl 37% by MallinckrodtAR®, C₂H₅OH (Avantor, 99%), C₁₅H₁₅N₃O₂ and C₁₄H₁₄N₃NaO₃S. Water was obtained using Purite® water purification system from the Research Center of Inorganic Materials and Complexes FMIPA Universitas Sriwijaya. The characterization of materials was performed using XRD Rigaku miniflex-6000. The functional groups were analyzed using FTIR Shimadzu Prestige-21 by the KBr method and sample was scanned at 400–4000 cm⁻¹. Adsorption-desorption of N₂ Analysis was measured using Quantachrome Micro-metric ASAP. The concentration of the dye was analyzed using UV-Visible Biobase BK-UV 1800PC spectrophotometer.

Synthesis of Mg/Cr LDH

Mg/Cr LDH was synthesized at pH 10 using the co-precipitation method. Mg(NO₃)₂·6H₂O (0.75 M in 100 mL) and Cr(NO₃)₃·9H₂O were mixed with a molarity ratio of 3:1 and was stirred for 1 hour. The solution of Na₂CO₃ was dropped to the reaction mixture then 2M NaOH was added until the mixture reached pH 10. The mixture was kept for 24 hours at 80°C under an N₂ atmosphere. The solid material was dried at 100°C overnight.

Preparation Mg/Cr LDH intercalated oxalate anion

Mg/Cr LDH was intercalated with oxalic anion by the ion exchange method. The mixture of 1 g of Mg/Cr LDH dissolved with water was stirred for 30 hours. As much as 5 g of oxalic acid was added to the mixture and then 4M of NaOH was added and pH was adjusted to 10. The reaction was kept for 3 days at 80°C under an N₂ atmosphere. The product of Mg/Cr-oxalate was filtered and dried at room temperature overnight

Adsorption study

The adsorption process was studied by variation of adsorption times, dyes concentrations, and temperatures. The variation of adsorption times were carried out at 5–150 minutes. The variation of dyes concentrations were conducted at 60, 70, 80, 90, and 100 mg/L. The variation of temperatures were studied at 303, 313, 323, and 333 K.

Desorption and regeneration experiment

The desorption process was conducted with water, sodium hydroxide, hydrochloric acid, and ethanol. As much as 5 g of adsorbent was added into 50 mL MR and MO (100 ppm) and stirred for 120 minutes. The adsorbent dried in an oven at 100°C for 2 hours. The dried adsorbent (0.02 g) was added into 20 mL solvent (water, sodium hydroxide, hydrochloric acid, and ethanol) for 120 minutes. The filtrate was measured by means of a UV-Vis spectrophotometer. The regeneration of adsorbent was performed after the adsorption desorption process. The adsorbent reuse was conducted for three cycles adsorption process.

RESULTS AND DISCUSSION

Characterization of Mg/Cr-LDH and intercalated Mg/Cr LDH with oxalate was carried out using XRD, BET, and FTIR analyses. The XRD characterization results are shown in Figure 2. Figure 2a is the diffraction pattern of Mg/Cr LDH, where there is a 2θ peak at angles 11°(003), 22°(006), 36°(115), and 60°(110) which indicates that the material has a layered structure (Palapa et al., 2020). Intercalated Mg/Cr LDH with oxalate anion has an XRD pattern that resembles Mg/Cr LDH. However, a shifting peak at 11° to 10° indicates an exchange of nitrate anions with oxalate (Giscard et al., 2016). The success of the intercalation process is supported by the data on increasing the interlayer distance from 7.62 Å on Mg/Cr LDH to 11.35 Å on intercalated Mg/Cr LDH.

The N₂ adsorption-desorption curve is presented in Figure 3. On the basis of the IUPAC classification, Mg/Cr LDH and Mg/Cr-oxalate in Figures 3a and b follow the type IV isotherm pattern. According to Mishra et al. (2018), type IV isotherm pattern shows mesoporous material and hysteresis occurs. The data resulting from the BET calculation is shown in Table 1 which shows the increase in the surface area of the material after intercalation with oxalate ions. It can be seen from intercalated Mg/Cr LDH which has a surface area of 49.27 m²/g after the intercalation process. However, Mg/Cr LDH has a pore size and pore volume greater than intercalated Mg/Cr LDH. According to Palapa et al. (2020), the decrease in pore size and volume after

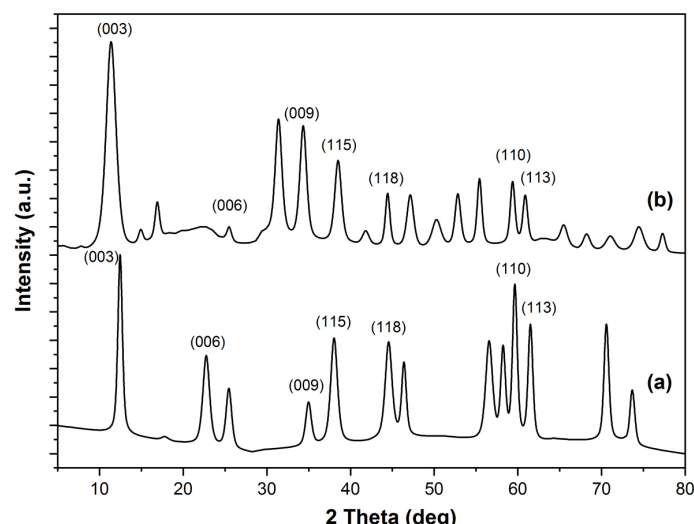


Figure 2. X-ray powder diffraction patterns of Mg/Cr LDH (a) and Mg/Cr-oxalate (b)

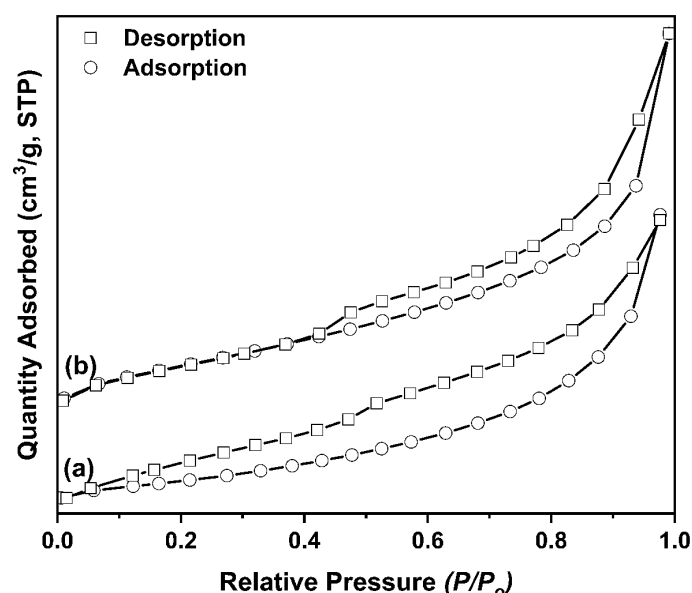


Figure 3. N₂ Adsorption-Desorption of Mg/Cr LDH (a) and Mg/Cr-oxalate (b) composites (c)

Table 1. BET Surface Area Analysis

Materials	Surface area (m ² /g)	Pore size (nm), BJH	Pore volume (cm ³ /g) _{BJH}
Mg/Cr LDH	21.511	3.20	6.564
Mg/Cr-oxalate	49.270	0.158	6.511

intercalation of Mg/Cr LDH is assumed due to oxalate ions covering the pores of the material after the intercalation process.

FTIR spectrum of Mg/Cr LDH and Mg/Cr-oxalate are presented in Figure 4. The vibration peaks of Mg/Cr LDH and Mg/Cr-oxalate are around 3448 cm⁻¹ and 1635 cm⁻¹ indicate the -OH stretching vibrations and bending vibration from water molecules. The vibration peak at wavenumber 1381 cm⁻¹ is assigned as the

vibration of the nitrate ion at Mg/Cr LDH. According to Giscard et al. (2016), the existence of an oxalate anion is confirmed by the presence of a vibrational peak around 1550 cm⁻¹ and 1365 cm⁻¹. A decrease in the peak of the vibration at wavenumber 1381 cm⁻¹ indicates that there has been an exchange of nitrate to oxalate ion on the interlayer.

The effect of the adsorption time of MR and MO using Mg/Cr LDH and Mg/Cr-oxalate

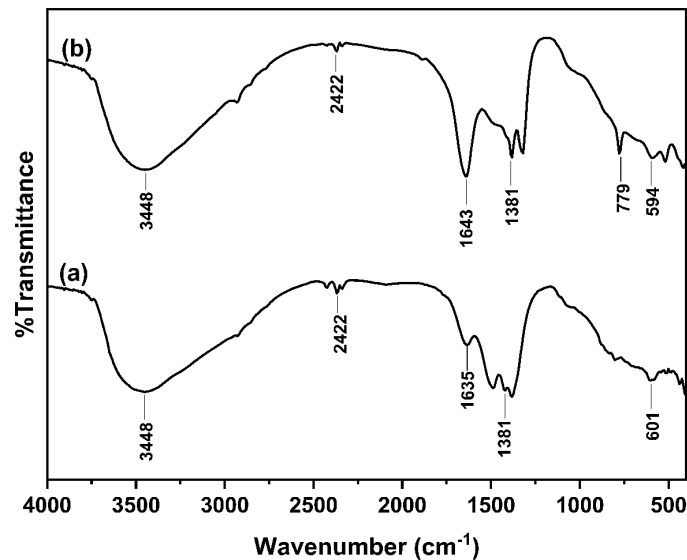


Figure 4. FT-IR Spectrum of Mg/Cr LDH (a) and intercalated Mg/Cr-oxalate (b)

is presented in Figure 5. The graph in Figure 5 shows that the adsorption process using Mg/Cr-oxalate absorbs higher than Mg/Cr LDH for both MR and MO dyes. This allows that the intercalation material has a large surface area value, thus adsorbent Mg/Cr-oxalate has a high ability to absorb dyes. Figure 5 also shows that the optimum time achieved by Mg/Cr LDH and Mg/Cr-oxalate to adsorb MR and MO was achieved at 100 minutes. The kinetic parameter data of the variation of adsorption time can be seen in Table 2.

The pseudo-first-order (PFO) and pseudo-second-order (PSO) kinetics model are determined from the R^2 value which is closer to one (David Kowanga et al., 2016). According to Li et al. (2012), the PFO kinetics model assumes the adsorption rate is influenced by the active site of the adsorbent, while PSO assumes that the

reaction process is influenced by the exchange or division of adsorbate and adsorbent. The data in Table 2 shows that the R^2 value of the PFO kinetics model for the adsorption process using each adsorbent is closer to 1 than PSO. Thus, the adsorption process takes place following the PFO kinetic model.

The data on the effect of concentration and temperature of MR and MO adsorption using Mg/Cr LDH and Mg/Cr-oxalate are presented in Figures 6 and 7. These figures shows that the increase in concentration is proportional to the increase in adsorption capacity. The MR adsorption process using Mg/Cr-oxalate (Fig. 6b) has a higher adsorption capacity of 63.291 mg/L than pristine adsorbent, while the MR adsorption capacity using Mg/Cr LDH was 53.476 mg/L. The same phenomenon was found for the MO

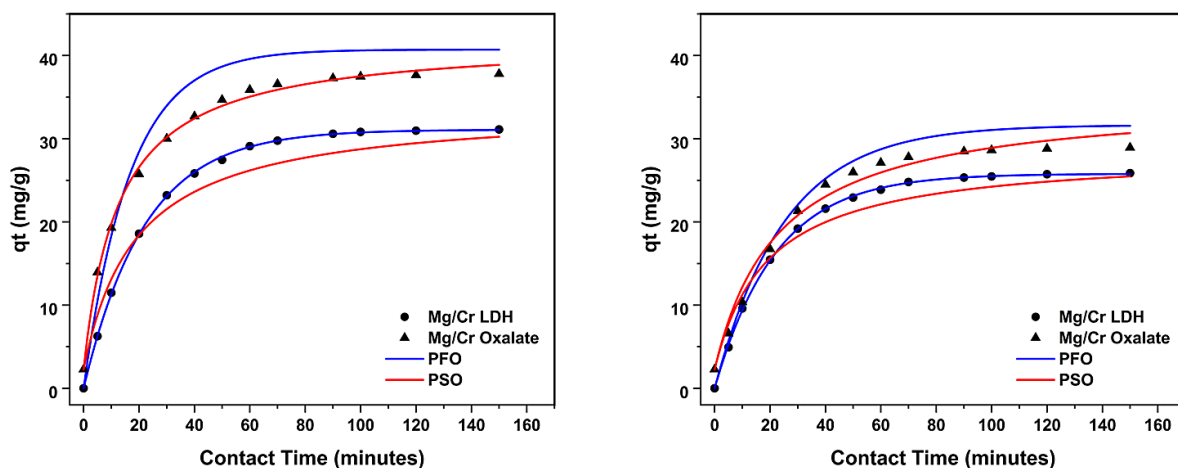


Figure 5. Time variation of adsorption MR and MO onto Mg/Cr LDH (a)

Table 2. Kinetic parameters of dyes adsorption onto Mg/Cr LDH and Mg/Cr-oxalate

Dye	Adsorbent	Q _{e,exp} (mg/g)	PFO			PSO		
			Q _{e,calc} (mg/g)	R ²	k ₁	Q _{e,calc} (mg/g)	R ²	k ₂
MR	Mg/Cr LDH	31.119	31.355	0.998	0.045	35.971	0.994	0.002
	Mg/Cr-oxalate	41.567	36.467	0.999	0.046	45.455	0.998	0.002
MO	Mg/Cr LDH	25.867	25.015	0.998	0.043	28.409	0.997	0.003
	Mg/Cr-oxalate	31.200	33.581	0.999	0.046	35.336	0.994	0.002

adsorption process. The adsorption capacity using Mg/Cr-oxalate was up to 53.191 mg/L and for Mg/Cr LDH was 41.841 mg/L. Intercalated Mg/Cr LDH material has a higher adsorption ability than the pristine one. This is supported by the surface area data from intercalated Mg/Cr LDH which is greater than Mg/Cr-LDH, which has been described above. The adsorption isotherm parameter for MR and MO on both adsorbents can be seen in Table 3.

The isotherm parameters studied in this research were the Langmuir and Freundlich models. Adsorption isotherms are used to study the mechanisms that take place during the adsorption process. The adsorption isotherm parameter is determined by an R² value that is close to one.

Table 3 shows that the R² value of the MR and MO adsorption process using Mg/Cr LDH and Mg/Cr-oxalate follows the Langmuir isotherm. The Langmuir isotherm model assumes that the adsorption process which takes place on the adsorbent surface is homogeneous. The Langmuir Isotherm explains that on the surface of the adsorbent there is an active site that is proportional to the surface area. Each active site has only one adsorbable molecule. This allows the adsorption to take place on a monolayer basis (Murtihapsari et al., 2017). The data in Table 3 shows that at high temperatures, the adsorption capacity increases. The maximum capacity of the adsorption process can be seen from the Q_{max} value. The Mg/Cr-oxalate adsorbent at a temperature of 333

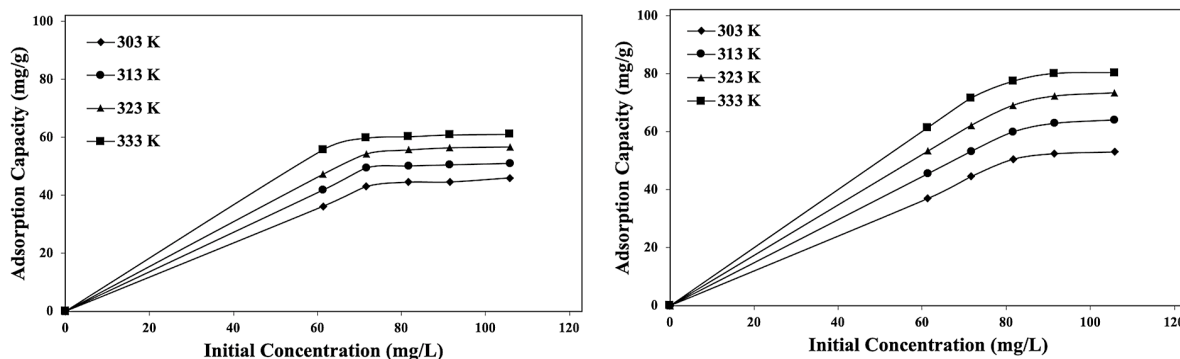


Figure 6. Effect of concentration and temperature on the adsorption of MR onto Mg/Cr LDH (a) and Mg/Cr-oxalate (b)

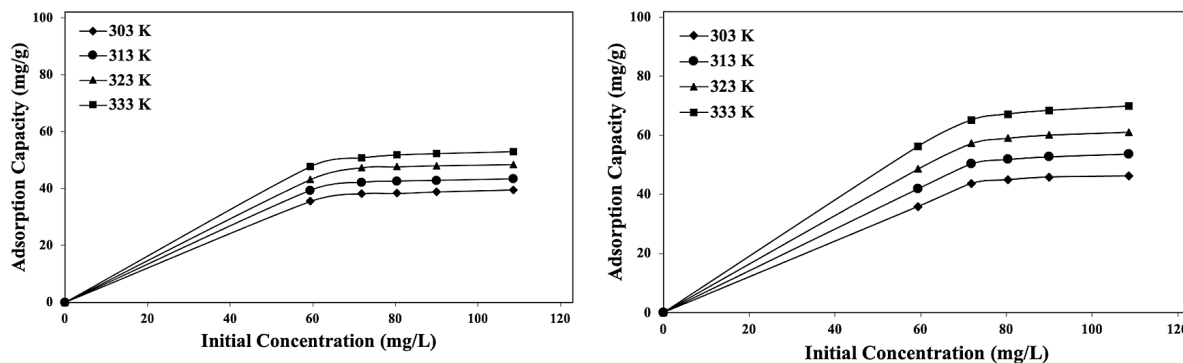


Figure 7. Effect of concentration and temperature on the adsorption of MO onto Mg/Cr LDH (a) and Mg/Cr-oxalate (b)

Table 3. Isotherms Parameter of Adsorption MR and MO on Mg/CrLDH and Mg/Cr-oxalate

Dye	Adsorbent	Adsorption isotherm	Adsorption constant	T (K)			
				303 K	313 K	323 K	333 K
MR	Mg/Cr LDH	Langmuir	Q_{max}	53.476	55.556	60.241	61.728
			k_L	0.110	0.235	0.373	1.906
			R^2	0.980	0.990	0.996	0.999
		Freundlich	n	1.132	2.941	2.381	5.650
	k_F		1.417	1.462	1.474	1.041	
	R^2		0.922	0.997	0.939	0.976	
	Mg/Cr-oxalate	Langmuir	Q_{max}	63.291	68.966	80.645	81.235
			k_L	0.105	0.322	0.325	0.590
R^2			0.977	0.999	0.993	0.999	
Freundlich		n	0.799	1.148	1.769	2.360	
	k_F	1.038	1.152	1.326	1.540		
	R^2	0.966	0.990	0.934	0.985		
MO	Mg/Cr LDH	Langmuir	Q_{max}	41.841	45.249	50.251	54.645
			k_L	0.262	0.392	0.477	0.620
			R^2	0.999	0.999	0.999	0.999
		Freundlich	n	1.931	2.732	3.731	2.320
			k_F	1.035	1.436	1.038	1.039
			R^2	0.941	0.996	0.997	0.965
	Mg/Cr-oxalate	Langmuir	Q_{max}	53.191	59.524	64.935	71.429
			k_L	0.125	0.193	0.390	1.296
			R^2	0.979	0.991	0.997	0.999
		Freundlich	n	1.098	1.193	1.464	2.415
			k_F	1.408	1.443	1.472	1.507
			R^2	0.991	0.983	0.982	0.997

K has the highest Q_{max} value for MR and MO adsorption. This proves that the intercalated material has a good ability in the adsorption process. Thermodynamic parameter data from the MR and MO adsorption process are presented in Tables 4 and 5, respectively.

The thermodynamic parameters studied in this research include ΔH , ΔS , and ΔG . A positive value on the change in ΔH indicates that the adsorption process is endothermic (Batool et al., 2018). according to Starukh & Levytska (2019), the range of enthalpy values at 40–120 kJ/mol is a chemisorption process. However, if the enthalpy has a value below that range, the adsorption process takes place physically. The thermodynamic parameter data from the MR adsorption process using Mg/Cr LDH and Mg/Cr-oxalate in Table 4 show a positive enthalpy value in the range of 10–60 kJ/mol. These results shows that the adsorption process occurs physically.

The ΔG value is used to determine the spontaneity of the adsorption process. A negative value indicates that the adsorption process was spontaneous while a positive value indicates a non-spontaneous process. The data in Table 4

shows the ΔG value of the MR adsorption process using either Mg/Cr-LDH or intercalated Mg/Cr LDH gives a negative value. These data indicates that the adsorption process was spontaneous (Ebelgi et al., 2020). Entropy (ΔS) is used to describe randomness on the surface of a material. A positive value of ΔS indicates an increase in randomness during the adsorption process (Belhamdi et al., 2016). The data in Table 4 shows a positive ΔS value and decreases as the adsorbate concentration increases.

The ΔH values in Table 5 for the MO adsorption process using Mg/Cr LDH show positive results and are in the range of 14–27 kJ/mol. This indicates that the adsorption process occurs physically. The negative value shown in the MO adsorption process using Mg/Cr LDH and Mg/Cr-oxalate proves that the adsorption process occurs spontaneously. Similar to the MR adsorption process, the MO adsorption process using Mg/Cr LDH and Mg/Cr-oxalate gives a positive Z value and decreases with increasing concentration.

The adsorption capacity of MR and MO in this research is slightly higher than various carbon

Table 4. Thermodynamic parameters of Adsorption MR onto Mg/CrLDH and Mg/Cr-oxalate

Concentration (mg/L)	T (K)	Mg/Cr-LDH			Mg/Cr-oxalate		
		ΔH (kJ/mol)	ΔS (kJ/mol)	ΔG (kJ/mol)	ΔH (kJ/mol)	ΔS (J/mol.K)	ΔG (kJ/mol)
61.343	303	52.075	0.174	-0.530	59.866	0.201	-0.944
	313			-2.266			-2.951
	323			-4.002			-4.958
	333			-5.738			-6.965
71.642	303	33.102	0.112	-0.972	56.324	0.190	-1.117
	313			-2.096			-3.013
	323			-3.221			-4.909
	333			-4.345			-6.805
81.642	303	23.983	0.081	-0.435	49.798	0.168	-1.126
	313			-1.241			-2.807
	323			-2.047			-4.487
	333			-2.853			-6.168
91.493	303	20.787	0.068	0.126	42.144	0.141	-0.620
	313			-0.555			-2.032
	323			-1.237			-3.443
	333			-1.919			-4.855
105.821	303	16.246	0.051	0.671	33.191	0.110	-0.009
	313			0.157			-1.104
	323			-0.357			-2.200
	333			-0.871			-3.296

Table 5. Thermodynamic parameters of Adsorption MO ontoMg/Cr LDH andMg/Cr-oxalate

Concentration (mg/L)	T (K)	Mg/Cr-LDH			Mg/Cr-oxalate		
		ΔH (kJ/mol)	ΔS (kJ/mol)	ΔG (kJ/mol)	ΔH (kJ/mol)	ΔS (J/mol.K)	ΔG (kJ/mol)
59.375	303	27.899	0.095	-0.892	66.620	0.222	-0.525
	313			-1.842			-2.741
	323			-2.792			-4.957
	333			-3.743			-7.173
71.875	303	21.534	0.072	-0.276	50.322	0.169	-0.796
	313			-0.996			-2.483
	323			-1.716			-4.170
	333			-2.436			-5.858
80.398	303	19.541	0.064	0.271	38.363	0.128	-0.434
	313			-0.365			-1.714
	323			-1.001			-2.995
	333			-1.637			-4.275
90.057	303	17.072	0.054	0.729	30.915	0.102	0.012
	313			0.189			-1.007
	323			-0.350			-2.027
	333			-0.889			-3.047
108.617	303	14.412	0.043	1.436	24.914	0.079	1.054
	313			1.007			0.266
	323			0.579			-0.521
	333			0.151			-1.309

based adsorbents, as shown in Table 6. Mg/Cr-oxalate after intercalation has higher adsorption capacity than pristine LDH under the same adsorption conditions.

The results of the MR and MO desorption process using Mg/Cr LDH andMg/Cr-oxalate

are presented in Figure 8. Figure 8a is the results of MR and MO desorption using Mg/Cr LDH. These data indicate that the HCl solvent provides the highest percentage of desorption, reaching 80.433% for MR and 97.973% for MO. On the basis of (Badri et al., 2021),

Table 6. Comparison of the adsorption capacity of MR and MO using several adsorbents.

Adsorbent	Adsorbate	Adsorption capacity (mg/g)	Reference
Carbon from the <i>Annona Squamosa</i> seed (CAS)	MR	81.970	[24]
Palladium nanoparticles on activated carbon		60.970	[25]
Hydroxyapatite		6.675	[26]
Banana pseudostem fibers		88.500	[27]
White potato peel powder		30.480	[28]
Modified chitosan		61.840	[29]
Activated carbon		46.290	[25]
Mg/Cr LDH		61.728	This research
Mg/Cr-oxalate		81.235	This research
Activated carbon		MO	370.360
Fe-Mg LDH	44.843		[31]
Cs-CaCl ₂	44.843		[31]
CTS/MMT	70.420		[32]
Fly ash	0.69		[33]
Sugar scum powder	15.24		[34]
Chitosan	34.830		[35]
Mg/Cr LDH	54.645		This research
Mg/Cr-oxalate	71.429		This research

Mg/Cr LDH is easier to exfoliate in acidic solvents. Hence, the adsorbate bound to the surface of Mg/Cr LDH is more easily desorbed. Similar to Mg/Cr LDH, for the desorption of Mg/Cr-oxalate on MR and MO it is more suitable to use HCl as a solvent. The results of

this desorption affect the regeneration process, which can be seen in Figure 9.

The results of this desorption affect the regeneration process, which can be seen in Figure 9. Regeneration of the Mg/Cr LDH and Mg/Cr-oxalate materials was carried out in three cycles. The

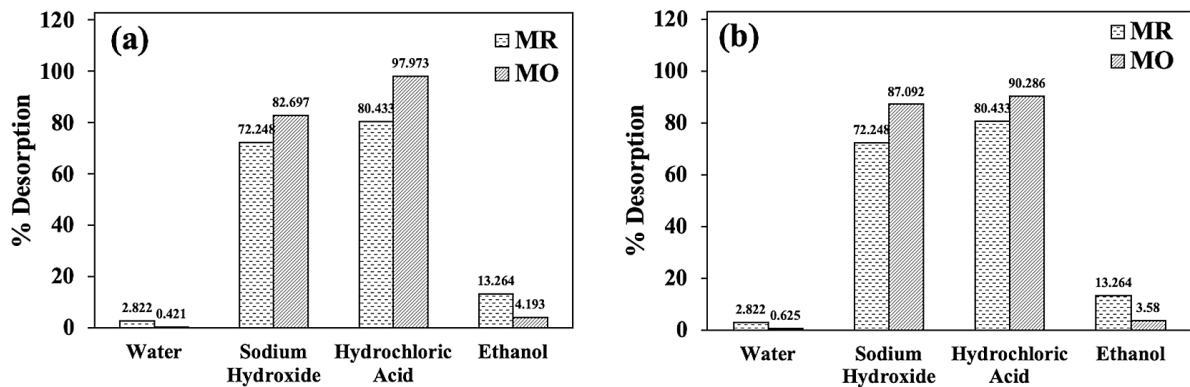


Figure 8. Desorption MR and MO on Mg/Cr LDH (a) and Mg/Cr-oxalate (b)

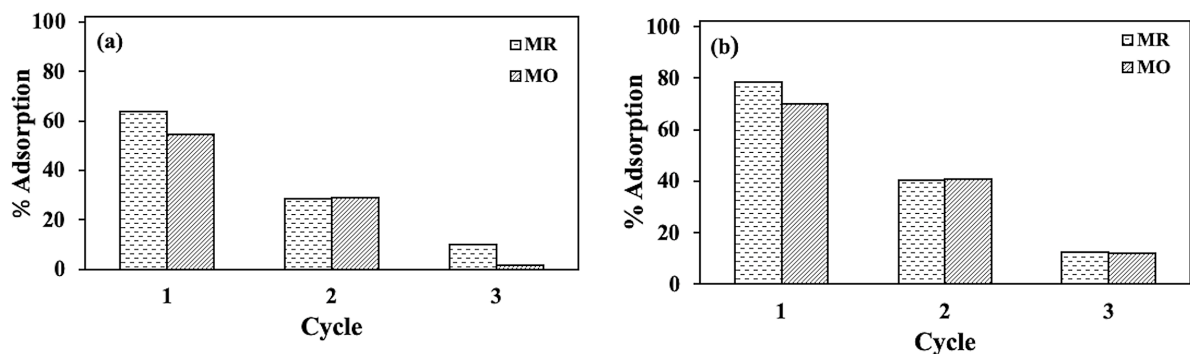


Figure 9. Regeneration MR and MO on Mg/Cr LDH (a) and Mg/Cr-oxalate (b)

Mg/Cr-oxalate adsorbent has a higher regeneration ability than Mg/Cr LDH. This phenomenon assumes that intercalated Mg/Cr LDH with oxalate has resistance to acid solvents. The regeneration ability of Mg/Cr LDH decreased drastically because it was exfoliated by the acid solvent.

CONCLUSIONS

The intercalation process of Mg/Cr LDH has been successfully carried out to form Mg/Cr-oxalate. The success of the intercalation process is supported by the XRD data, which shows an increase in the interlayer distance from 7.62 Å to 11.35 Å and a significant increase in the surface area reaching 49.270 m²/g. MR adsorption capacity using Mg/Cr LDH and Mg/Cr-oxalate reached 61.728 mg/g and 81.325 mg/g, respectively, while the MO adsorption capacity reached 54.645 mg/g and 71.429 mg/g for each adsorbent. MR and MO adsorption followed the PFO kinetics model. On the other hand, the thermodynamic parameters of the MR and MO adsorption processes take place endothermic and spontaneously. The regeneration results show that Mg/Cr-oxalate is reusable because it is more resistant to acidic solvents toward a desorption process.

Acknowledgements

Universitas Sriwijaya for financial support of this research through Hibah Profesi in fiscal year 2020/2021 contract No. SP DIPA-023.17.2.677515/2020 for additional output-based research and also to Research Center of Inorganic Materials and Complexes FMIPA Universitas Sriwijaya for instrumental and analysis support.

REFERENCES

1. Ai, L., Zhang, C., Meng, L. 2011. Adsorption of methyl orange from aqueous solution on hydrothermal synthesized Mg-Al layered double hydroxide. *Journal of Chemical and Engineering Data*, 56, 4217–4225.
2. Amelia, S., Maryudi, M. 2019. Application of natural zeolite in methylene blue wastewater treatment process by adsorption method. *Jurnal Bahan Alam Terbarukan*, 8, 144–147.
3. Badri, A.F., Palapa, N.R., Mohadi, R., Lesbani, A. 2021. Mg-Cr layered double hydroxide with intercalated oxalic anion for removal cationic dyes

rhodamine B and methylene blue. *Journal of Environmental Treatment Techniques*, 9, 85–94.

4. Batool, F., Akbar, J., Iqbal, S., Noreen, S., Bukhari, S.N.A. 2018. Study of isothermal, kinetic, and thermodynamic parameters for adsorption of cadmium: an overview of linear and nonlinear approach and error analysis. *Bioinorganic Chemistry and Applications*, 2018.
5. Belhamdi, B., Merzougui, Z., Trari, M., Addoun, A. 2016. A kinetic, equilibrium and thermodynamic study of L-phenylalanine adsorption using activated carbon based on agricultural waste (date stones). *Journal of Applied Research and Technology*, 14, 354–366.
6. Benkhaya, S., M'rabet, S., El Harfi, A. 2020. Classifications, properties, recent synthesis and applications of azo dyes. *Heliyon*, 6.
7. Imron, M., Said, M. 2017. Adsorption of procion red using layer double hydroxide Mg/Al. *Science and Technology Indonesia*, 2, 64–67.
8. David Kowanga, K., Omare Mauti, G., Mbaka Mauti, E., Gatebe, E. 2016. Kinetic, sorption isotherms, pseudo-first-order model and pseudo-second-order model studies of Cu(II) and Pb(II) using defatted Moringa oleifera seed powder. *The Journal of Phytopharmacology*, 5, 71–78.
9. Ebelgi, A.N., Ayawei, N., Wankasi, D. 2020. Interpretation of adsorption thermodynamics and kinetics. *Open Journal of Physical Chemistry*, 10, 166–182.
10. Vinsiah, R., Mohadi, R., Lesbani, A. 2017. Performance of graphite for congo red and direct orange adsorption. *Indonesian Journal of Environmental Management and Sustainability*.
11. Giscard, D., Kamgaing, T., Temgoua, R.C.T., Ymele, E., Tchieno, F.M.M., Tonlé, I.K. 2016. Intercalation of oxalate ions in the interlayer space of a layered double hydroxide for nickel ions adsorption. *International Journal of Basic and Applied Sciences*, 5, 144.
12. Hassaan, M.A., Nemr, A.E. 2017. Health and environmental impacts of dyes: Mini review. *American Journal of Environmental Science and Engineering*, 1, 64–67.
13. He, X., Qiu, X., Hu, C., Liu, Y. 2018. Treatment of heavy metal ions in wastewater using layered double hydroxides: A review. *Journal of Dispersion Science and Technology*, 39, 792–801.
14. Li, H. qin, Huang, G. he, An, C. jiang, Zhang, W. xiang. 2012. Kinetic and equilibrium studies on the adsorption of calcium lignosulfonate from aqueous solution by coal fly ash. *Chemical Engineering Journal*, 200–202, 275–282.
15. Mishra, G., Dash, B., Pandey, S. 2018. Layered double hydroxides: A brief review from fundamentals to application as evolving biomaterials. *Applied Clay Science*, 153, 172–186.
16. Murtihapsari, M., Mangallo, B., Handyani, D.D. 2017. Model isotherm freundlich dan langmuir oleh

- adsorben arang aktif bambu andong (*G. verticillata* (Wild) Munro) dan bambu ater (*G. atter* (Hassk) Kurz ex Munro). *Jurnal Sains Natural*, 2, 17.
17. Palapa, N.R., Taher, T., Rahayu, B.R., Mohadi, R., Rachmat, A., Lesbani, A. 2020. CuAl LDH/Rice Husk Biochar Composite for Enhanced Adsorptive Removal of Cationic Dye from Aqueous Solution. *Bulletin of Chemical Reaction Engineering & Catalysis*, 15, 525–537.
 18. Rathee, G., Awasthi, A., Sood, D., Tomar, R., Tomar, V., Chandra, R. 2019. A new biocompatible ternary Layered Double Hydroxide Adsorbent for ultrafast removal of anionic organic dyes. *Scientific Reports*, 9, 1–14.
 19. Rubia, Bhardwaj, A. 2016. International journal of engineering sciences & research technology. *International Journal of Engineering Science and Research*, 5, 778–781.
 20. Semeraro, P., Fini, P., D'Addabbo, M., Rizzi, V., Cosma, P. 2017. Removal from wastewater and recycling of azo textile dyes by alginate-chitosan beads. *International Journal of Environment, Agriculture and Biotechnology*, 2, 1835–1850.
 21. Shan, R. ran, Yan, L. guo, Yang, Y. ming, Yang, K., Yu, S. jun, Yu, H. qin, Zhu, B. cun, Du, B. 2015. Highly efficient removal of three red dyes by adsorption onto Mg-Al-layered double hydroxide. *Journal of Industrial and Engineering Chemistry*, 21, 561–568.
 22. Starukh, H., Levytska, S. 2019. The simultaneous anionic and cationic dyes removal with Zn–Al layered double hydroxides. *Applied Clay Science*, 180, 1–5.
 23. Taher, T., Christina, M.M., Said, M., Hidayati, N., Ferlinahayati, F., Lesbani, A. 2019. Removal of iron(II) using intercalated Ca/Al layered double hydroxides with [-SiW₁₂O₄₀]⁴⁻. *Bulletin of Chemical Reaction Engineering Catalysis*, 14, 260–267.
 24. Zhao, G., Liu, L., Li, C., Zhang, T., Yan, T., Yu, J., Jiang, X., Jiao, F. 2018. Construction of diatomite/ZnFe layered double hydroxides hybrid composites for enhanced photocatalytic degradation of organic pollutants. *Journal of Photochemistry and Photobiology A: Chemistry*, 367, 302–311.